

Micro & strong lensing with the Square Kilometer Array: The mass-function of compact objects in high-redshift galaxies

L.V.E. Koopmans

Kapteyn Astronomical Institute

P.O.Box 800

NL-9700 AV Groningen

The Netherlands

E-mail: leon@astro.rug.nl

A.G. de Bruyn

Netherlands Foundation for Research in Astronomy

P.O. Box 2

7990 AA Dwingeloo

The Netherlands

E-mail: ger@nfra.nl

We present the results from recent VLA 8.5-GHz and WSRT 1.4 and 4.9-GHz monitoring campaigns of the CLASS gravitational lens B1600+434 and show how the observed variations argue strongly in favor of microlensing by MACHOs in the halo of a dark-matter dominated edge-on disk galaxy at $z=0.4$. The population of flat-spectrum radio sources with micro-Jy flux-densities detected with the *Square-Kilometer-Array* is expected to have dimensions of micro-arcsec. They will therefore vary rapidly as a result of Galactic scintillation (diffractive and refractive). However, when positioned behind distant galaxies they will also show variations due to microlensing, even more strongly than in the case of B1600+434. Relativistic or superluminal motion in these background sources typically leads to temporal variations on time scales of days to weeks. Scintillation and microlensing can be distinguished, and separated, by their different characteristic time scales and the frequency dependence of their modulations. Monitoring studies with *Square-Kilometer-Array* at GHz frequencies will thus probe both microscopic and macroscopic properties of dark matter and its mass-function as a function of redshift, information very hard to obtain by any other method.

1 Introduction

Gravitational lens (GL) systems offer a versatile tool to study a range of cosmological and astrophysical problems. One of most puzzling and difficult problems to solve in all of astrophysics, is that of the distribution and nature of dark-matter. Paczynski [14] suggested to search for one of the dark-matter candidates – i.e. massive compact objects, possibly stellar remnants or primordial black holes – using their gravitational lensing effect on background stars. Many so called microlensing surveys have been undertaken since then, with varying success [12].

One major disadvantage of these Galactic microlensing surveys is the low microlensing optical depth ($\tau \sim 10^{-6}$) [1]. In multiply-imaged GL systems $\tau \sim 1$, making them much more suitable to search for microlensing variability (e.g. [19]). The major disadvantage in this case is the long variability time scale, which can amount to many years. This is especially true if the lens galaxy is at a high redshift *and* the velocity of the microlensing magnification pattern is dominated by the velocity of the compact objects with respect to the line-of-sight to the stationary optical source.

What about microlensing in the radio? Most sources are much more extended in the radio than in the optical. It is therefore often believed that they are nearly unaffected by microlensing. However, many flat-spectrum radio sources contain jet-components moving with near or superluminal velocity. These components can be as small as several μas at the mJy level, to sub- μas

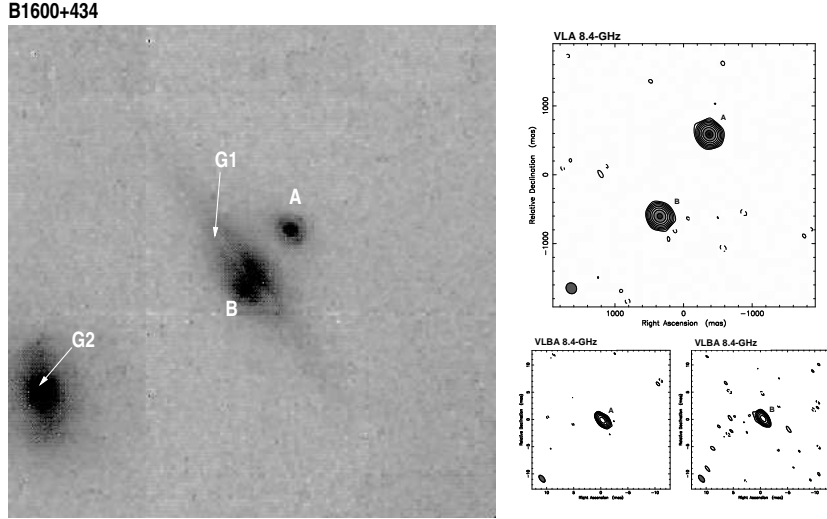


Figure 1: **Left:** HST NICMOS H-band image of B1600+434, showing the two lens images (A and B), the edge-on spiral lens galaxy (G1) and a companion galaxy (G2). Lens image B passes predominantly through the disk/bulge of the spiral galaxy. Image A, however, passes exclusively through its dark-matter halo and is therefore *only* susceptible to microlensing by MACHOs, making B1600+434 a unique target for this purpose. **Right:** Top: VLA 8.5-GHz A-array image of B1600+434. Bottom: VLBA 8.5-GHz images of the lens components B1600+434 A and B. Both lens images show no sign of any extended structure larger than ~ 1 mas.

at the μJy level. This is comparable or even smaller than the angular scale over which the microlensing magnification pattern changes significantly. Thus, at these levels radio microlensing can become important.

In Sections 2–4, we will illustrate the above with the CLASS GL B1600+434. In Sect.5, we will show how the *Square Kilometer Array* can improve this in the future.

2 The edge-on spiral lens system CLASS B1600+434

The gravitational lens B1600+434 [7] consists of a 1.4-arcsec double, lensed by a foreground edge-on spiral galaxy (Fig.1; [8] [9]), The lens galaxy and source are at redshifts of 0.41 and 1.59, respectively [4]. B1600+434 was discovered in the *Cosmic Lens All-Sky Survey* (CLASS), whose mission is to find multiply imaged flat-spectrum radio sources [2]. Early VLA and WSRT radio observations already indicated that the source was variable and therefore suitable for determining a time delay [9]. In the coming paragraphs, we shortly describe constraints on the mass model of the lens galaxy and the time delay between the lens images. Subsequently, we show that most of the short-term variability found in the radio light curves of the lens images is of external origin.

Mass models: In [9] a range of mass models to describe the edge-on disk galaxy (Fig.1) were presented, with the aim of constraining the dark-matter halo around the lens galaxy. A lower limit of $q_h \geq 0.5$ was found for the oblateness of the dark-matter halo. Moreover, at least half of the mass inside the Einstein radius must be contributed by the dark-matter halo, i.e. the maximum-disk hypothesis does not apply for this galaxy. Assuming an isothermal halo model, a time delay of about $54h_{50}^{-1}$ days was predicted in a flat FRW universe with $\Omega_m = 1$. The steeper MHP mass model for the dark matter halo predict a time delay of about $70h_{50}^{-1}$ days. Once the time delay between the lens images has been determined, constraints on the Hubble parameter can be set. However, more interesting, once the Hubble parameter can be determined from several other JVAS and CLASS lens delays, as well as other methods, the problem can be reversed and constraints can be put on the mass profile of the dark-matter halo around the edge-on spiral lens galaxy [9] [10].

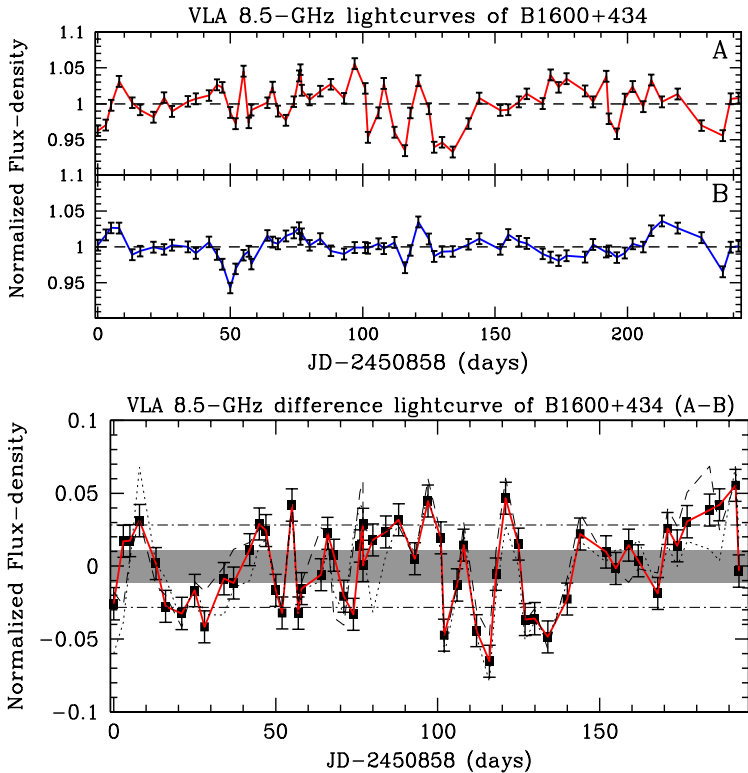


Figure 2: **Top:** The normalized light curves of B1600+434 A (upper) and B (lower), corrected for a long-term gradient. The error on each light-curve epoch is 0.7 to 0.8%. **Bottom:** The normalized difference light curve between the two lens images, corrected for both the time-delay (47d) and flux density ratio (1.212). The shaded region indicates the expected $1\text{-}\sigma$ (1.1%) region if all variability were due to measurement errors. The dash-dotted lines indicate the observed modulation index of 2.8%. The dotted and dashed curves indicate the normalized difference curves for a time delay of 41 and 52 days, respectively.

Time-Delay: A monitoring campaign was initiated in Febr. 1998 with the VLA in A- and B-arrays at 8.5-GHZ [10]. B1600+434 was observed on average every 3.3 days. The radio maps have S/N-ratios of ~ 300 and a resolution of typically 0.2 (0.7) arcsec in A (B) array (Fig.1). The final error on the calibrated flux densities of the lens images is 0.7–0.8%, dominated by the uncertainties in the flux-density calibration. The normalized calibrated light curves of both images are shown in Fig.2. A 15–20% long-term decrease in flux density of both images is seen over the observing period of eight months, most likely intrinsic source variability [10]. One also sees short term (days to weeks) variability of up to 10% peak-to-peak in image A, whereas the short term variability in image B is significantly less (Fig.2). We determined the time delay by scaling the observed light-curve B by the intrinsic flux-density ratio (1.212) and shifting it back in time, until the dispersion between the two image light curves minimized. We find a time delay of $\Delta t_{B-A} = 47_{-9}^{+12}$ days (95% confidence; [10]). The statistical error was determined from Monte-Carlo simulations and a maximum systematic error of $-8/+7$ days was estimated. Note that this method would have yielded a delay even if the source had not shown any short-term variability!

External variability: Once the time delay and flux-density ratio have been determined, the light curves can be subtracted to see if any significant variability is left. In Fig.2 the normalized difference light curve for B1600+434 is shown, using a time delay of 47 days and a flux-density ratio of 1.212. The difference light curve has an rms scatter of 2.8%, which is inconsistent with a flat difference light curve at the $14.6\text{-}\sigma$ confidence level [11]. The individual normalized light curves (i.e. the light curves divided by a linear fit) of images A and B (Fig.2) have rms variabilities of 2.8% and 1.6%, respectively. Both are significantly above the 0.7–0.8%, expected on the basis of measurement errors.

3 Radio Microlensing by MACHOs in B1600+434?

Below we investigate both scintillation and microlensing, as plausible causes of the external variability in the lens images of B1600+434 [11].

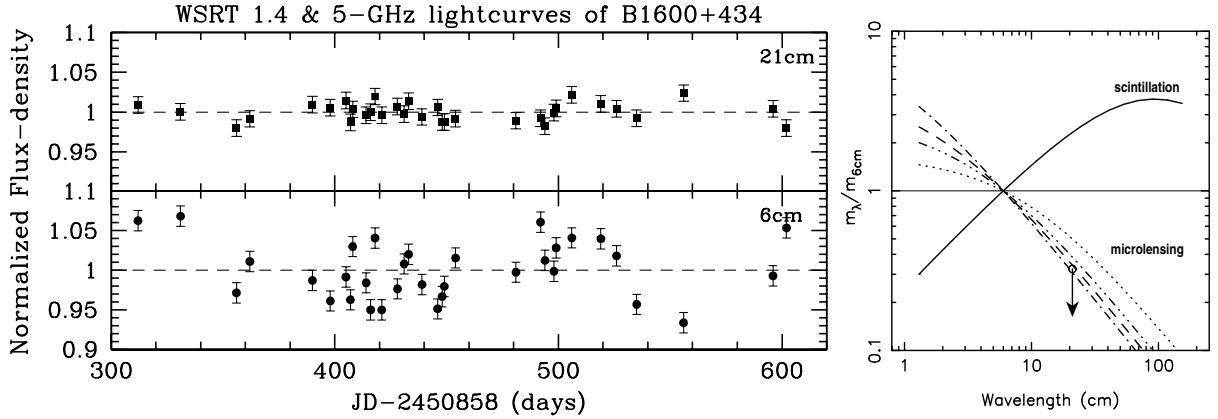


Figure 3: **Left:** The normalized WSRT 1.4 and 5-GHz flux-density light curves of B1600+434. Only those epochs of the WSRT light curves are shown that have both a 1.4 and 5-GHz measurement. One notices a clear increase in the modulation index from 21 to 6 cm by a factor ~ 3 . **Right:** Dependence of the modulation index from scintillation and microlensing on wavelength. The solid line shows the modulation index from scintillation. The broken lines show the modulation indices from microlensing for several microlensing models, constrained by the VLA 8.5-GHz light curves. All curves are normalized to the modulation index at 6.0 cm observed with the WSRT in 1999. The open circle indicates the observed modulation index at 21 cm, agreeing remarkably well with that predicted from microlensing.

Scintillation: Scintillation, caused by the Galactic ionized ISM, can explain both large amplitude variability in very compact extra-galactic radio sources and lower amplitude ‘flicker’ of more extended sources (e.g. [15]). In B1600+434-A and B, we observe several percent rms variability, possibly consistent with ‘flickering’. The time scale is harder to quantify, but it appears that we see variability time scales of several days up to several weeks (Fig.2).

Let us summarize the arguments that argue against scintillation: (i) The modulation index between the lens images differs, even though one looks at the same background source. This requires significantly different properties of the Galactic ionized ISM over scales of $1.4''$. (ii) Ongoing multi-frequency VLA and WSRT show a decrease in the modulation index with wavelength (Fig.3), whereas the opposite is expected for scintillation. (iii) A modulation index of a few percent corresponds to a variability time scale of less than 1–2 days for weak and strong refractive scattering, whereas variability over much longer scales seems to be present.

Although the difference in modulation index can be explained by considerable scatter-broadening of image B in the lens galaxy, all evidence put together build a considerable case against scintillation.

Microlensing: There are several good reasons why microlensing is a good explanation for the external variability that is observed in B1600+434: (i) Because B1600+434 is multiply imaged, the lens images pass through a foreground lens galaxy with microlensing optical depths near unity. Combined with the fact that many core-dominated flat spectrum radio source have superluminal jet-structure (e.g. [18]), makes it probable that microlensing variability is occurring at some level on time scales of weeks to months. (ii) From microlensing simulations [11], we find that a core plus a single superluminal knot can explain the rms and time scale of variability in the lens images. For image A, however, we require an average mass of compact objects $\geq 0.5-M_{\odot}$ to explain its significantly higher rms variability. More complex jets, with multiple components, would of course show reduced modulations, but this can then be compensated by making them somewhat smaller (i.e. a larger Doppler boosting). We have tested this, by replacing the simple source with a real jet-structure (i.e. 3C120), and shown that also more complex sources give observable microlensing variations in their light curves. (iii) The apparent decrease in rms variability (i.e. modulation index) with wavelength appears in agreement with a microlensed synchrotron self-absorbed source that grows proportional with wavelength (Fig.3).

The current observations are all in agreement with the microlensing hypothesis, even though

some of the short-term variability maybe due to scintillation [11]. In fact, objects compact enough to be microlensed should show scintillation at some level. In the case of microlensing, caustic crossings can brighten objects orders of magnitude more than scintillation if the emitting region is significantly smaller than the Fresnel scale of several μas at 8.5-GHz. In this case we expect variability to be dominated by microlensing.

4 B1600+434: Thus far...

We have presented the first *unambiguous* case of external variability of an extra-galactic radio source, the CLASS gravitational lens B1600+434 [11]. Several lines of evidence indicate that it is not dominated by scintillation, but by microlensing (in the lens galaxy) of a superluminal source. This requires a population of MACHOs in the halo around the edge-on disk galaxy with masses $\geq 0.5 M_{\odot}$. The discovery of a population of these objects might well indicate that its dark-matter halo mostly consists of stellar remnants. Maybe these objects are the (white) dwarfs as seen in the Hubble Deep Field [6] [13]. Our ongoing multi-frequency WSRT (Fig.3) and VLA observing campaigns should further tighten the constraints on this tantalizing possibility.

5 Future possibilities with the Square Kilometer Array

Above we have shown an example of the current possibilities of studying strong and microlensing in the radio. Preferably, one would like to monitor these systems simultaneously at many different frequencies and with much higher sensitivity. Although, we have started a multi-frequency campaign of B1600+434 with the VLA, we are working at the limits of present day technology.

The *Square Kilometer Array* (SKA) has sensitivities of sub- μJy levels after a few minutes of integration, a resolution of $\leq 0.1''$ at 20 cm and bandwidths around half a GHz (see [16]). With this sensitivity and the large instantaneous field of view (FOV; around $1^{\circ} \times 1^{\circ}$ at 20 cm), SKA would detect ≥ 100 radio sources per square arcmin (Fig.4; see also Hopkins et al, this volume). To estimate the number of GL system, useful for particular research projects, we use the following formula:

$$N = \text{FOV} \times n_r \times r_{\text{gl}} \times f_{\text{r-type}} \times f_{\text{g-type}}, \quad (1)$$

where FOV is the field-of-view, n_r is the number-density of radio source on the sky, r_{gl} is the strong-lensing rate of these sources, and $f_{\text{r-type}}$ and $f_{\text{g-type}}$ are the fractions of radio-sources and lens-galaxies with properties that one is interested in, respectively. Using either the lensing rate in the Hubble Deep Field, which has a comparable depth and number-density of objects, or the typical lensing rate for high- z sources of about $\leq 10^{-3}$, every synthesis observation with SKA contains a few hundred to one thousand GL systems. About 10% of these radio sources are expected to have compact structure [5], which will be easier to identify than the lensed starburst systems which dominate the source counts at μJy levels. However, even identifying the fainter cousins of the CLASS survey, will still be a major task, with the typical distance between radio sources being $\sim 6''$, and not having the benefit of equally large optical images to identify the lensing galaxies. However quad-configurations and variability will be very helpful.

What to do with that many GL systems? Below we discuss two projects, which we think might still be worth doing in ~ 10 years time (i.e. the development and implementation time-scale for SKA), although there will undoubtedly be many more projects.

Galaxy structure & evolution at high redshifts: To study the structure & evolution of galaxies up to very high redshifts, one would preferably have both their colors *and* mass-distribution. Colors can nowadays be obtain with instruments such as HST and ground-based 8/10-m class telescopes. However, obtaining information on the mass distribution of a significant sample of high-redshift galaxies is and will remain exceedingly difficult in the near future. This is especially true for spiral galaxies. For example, to obtain a decent sample of spiral galax-

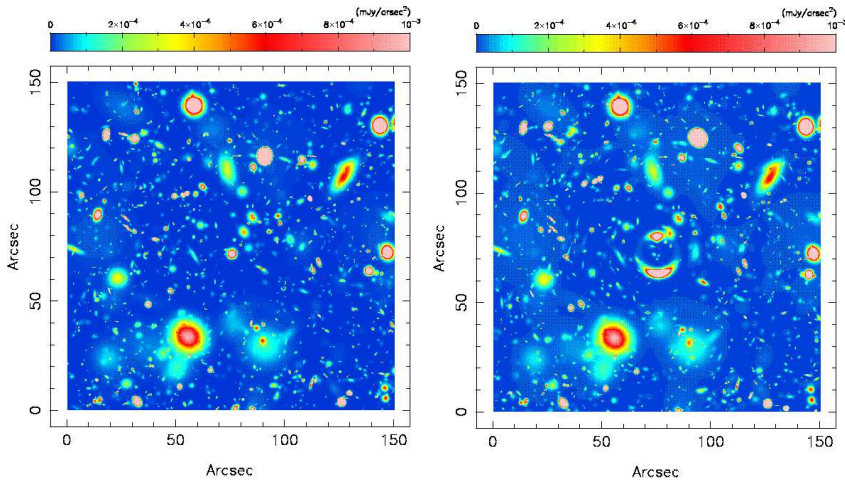


Figure 4: Left: Simulation of a $150'' \times 150''$ field, as could be observed with the Square Kilometer Array in a single 12-h integration at $\lambda=20$ cm (see also Hopkins et al, this volume). The shown FOV is comparable to that of the Hubble Deep Field. The real FOV of SKA at this wavelength will be around $1^\circ \times 1^\circ$. Right: The same, with a massive cluster (not shown) at $z=0.5$, lensing the background.

ies with detailed information on their mass distribution, one would like to have Einstein–ring type GL systems (like B0218+357), which provide considerable information on the mass distribution of the lens galaxy. Taking a fraction of $\sim 15\%$ for the expected fraction of spiral–lens galaxies, $\geq 50\%$ for the fraction of extended radio sources (i.e. larger than the Einstein radius), $n_r \approx 100$ per sq. arcmin and $r_{GL} = 10^{-3}$, we expect ~ 30 or more spiral–lens galaxies with radio Einstein rings per FOV! Not only can these Einstein–ring structures be used to constrain the mass distributions of these spiral galaxies, they can also be used to probe the HI content of the galaxy through absorption–line measurements, simultaneously constraining their velocity fields. Especially HI–absorption against lensed extended background radio sources would be very informative (e.g. PKS1830-211; [3]).

Constraining the mass-function of compact objects in high–redshift galaxies: As in the case of B1600+434, multi-frequency radio monitoring of those lensed sources which are compact and flat-spectrum, would allow one to separate variability resulting from strong and weak scattering by the ISM, plasma lensing and microlensing. Time delays can be determined, allowing one to determine the difference light curve between lens images. This is the only unambiguous method to separate intrinsic from non–intrinsic variability. How important this will turn out to be remains to be seen.

About 10% percent of all disk–lens systems is expected to lie within 5 degrees of edge-on. In fact, the CLASS/JVAS radio–GL survey has so far discovered at least 17 new lens systems, of which B1600+434 is one. One can therefore expect $\sim 5\%$ of all GL to be of this type. Assuming that $\sim 10\%$ of all radio sources are compact and flat–spectrum, a few of these systems could be detected with SKA for every FOV (~ 1 sq. degree). That is, a survey with SKA could detect ~ 10 of these systems per day. How could we use these systems to learn about the mass function of compact objects in their halo?

The study of variability in the lens images of these systems, as a function of height above the disk of the lens galaxy, could provide unique information on the composition of their dark–matter halos. Although most lens systems would be expected to lie at redshifts between 0.3 and 1, a fraction of $\sim 5\%$ will be found at redshifts ≥ 1.5 , allowing the study of the redshift dependence of dark matter halos.

Because with SKA one is looking at sources at the μJy level, the expected angular size of these radio sources is

$$\Delta\theta \approx \sqrt{\frac{S_{\mu\text{Jy}}}{T_{12}} \left(\frac{\lambda}{25\text{cm}}\right)^2} \mu\text{as}, \quad (2)$$

where T_{12} is the brightness temperature of the source in units of 10^{12} K. If the source is has a redshift z and Doppler–boosting factor \mathcal{D} , one should replace T_{12} with $\mathcal{D} T_{12}/(1+z)$.

Many compact flat–spectrum radio sources at high redshifts contain superluminal components,

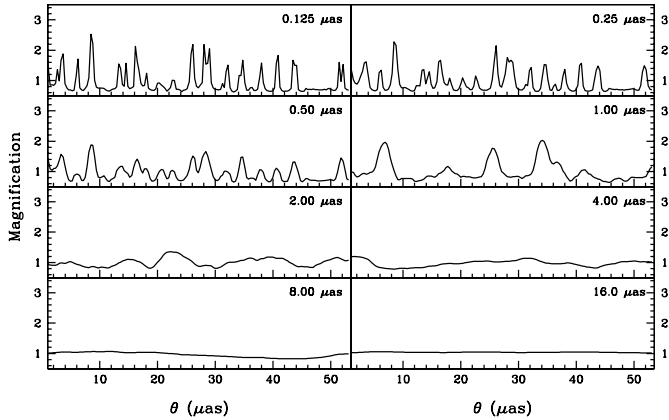


Figure 5: Arbitrary examples of simulated microlensing light curves, showing the dependence on source size. Whereas in the case of B1600+434, we are looking at jet-components of $\geq 2 \mu\text{as}$, SKA will be looking at sources with $\Delta\theta \ll 1 \mu\text{as}$. The gain in picking up microlensing induced variability is immediately obvious.

with \mathcal{D} of order a few. For example, a superluminal $0.1 \mu\text{Jy}$ jet-component with $\mathcal{D} \sim 10$ in a radio source at $z=2$ can be as small as $0.15 \mu\text{as}$ (with $T_{12} \approx 1$), which is much smaller than the Einstein radius of a $1-M_{\odot}$ compact object at intermediate redshift! We still do not know whether the radio-faint AGN will also show superluminal motion. On the other hand, much fainter galactic sources also show superluminal motion. Such a component moving with superluminal velocity over a microlensing magnification pattern will show up in the image lightcurves as variability of up to many tens of percents on time scales of months, weeks and maybe even days. Because of the compactness of these jet-components, the variability in their light curves, induced by microlensing, will almost perfectly trace the magnification pattern due to the compact objects, as is the case in the optical (Fig.5).

Moreover, for superluminal sources the microlensing time-scale is not dominated by the velocity of the compact lens objects (few hundred km/s), but by the velocity of the jet-component ($\geq c$). Hence, not only the variability time-scale is compressed by a factor $\geq 10^3$, also the microlensing rate will enormously increase [17]. Flat-spectrum radio sources could therefore be the perfect probes to study compact objects and their mass function in galaxies up to high redshifts!

However, how can one separate microlensing, scintillation and intrinsic variability of these sources? First, scintillation takes place on time-scales of \leq few hours for these ultra-compact sources. By averaging over longer time scales one can easily remove this, leaving only microlensing and intrinsic variability. Subtracting the averaged light curves of the different lens images, as for B1600+434, will subsequently remove intrinsic variability. The difference light curve that remains *only* contains microlensing variability. Second, both microlensing and scintillation are strongly dependent on frequency. Whereas microlensing increases with frequency, because the source becomes more compact (eqn.2), scintillation will decrease, because of the frequency-dependent refractive properties of the Galactic ionized ISM (e.g. Fig.3). The scintillation is of course strongest around the transition frequency from weak to strong, about 5 GHz. At longer wavelengths, e.g. 21cm, very fast diffractive scintillation could also become important for sub-microarcsecond sources. The large bandwidth of SKA ($\Delta\nu \sim \nu/2$), however, will allow one to further discriminate between microlensing and the different types of scintillation.

In the case of B1600+434, separating properties of the source and mass-function is complicated. In the case of very compact sources, which will be observed with SKA, this is less problematic. As mentioned before, these sources are usually much smaller than the angular scale over which the magnification pattern changes significantly. In other words, one can often regard the source as a point source, which clearly simplifies unraveling the source and mass-function properties. The statistical properties of the difference light curves can thus be used to study the mass function of compact objects at those positions where the lens images pass through the lens galaxy (e.g. halo, disk or bulge).

Microlensing studies, of course, would not have to be confined to multiply-imaged radio sources. Detailed multi-frequency studies of suitable alignments of compact radio sources and foreground galaxies could be used to study the properties of lensing matter as a function of distance to the

galaxy out to any distance, far into its dark-matter halo! A statistical study of the frequency-dependent modulation characteristics as a function of distance to the foreground galaxy can also be used to separate galactic scintillation from microlensing because the galactic ISM is not expected to change rapidly on angular scales of a few arcseconds.

6 Conclusions

Illustrated by the GL system B1600+434, we have shown the current limitations, but also the exciting possibilities of detecting compact objects in the dark-matter halo of intermediate-redshift galaxies and constraining their mass function through radio microlensing.

The *Square Kilometer Array* will be two orders of magnitude more sensitive than the current VLA, and, because of multi-beaming, an additional order of magnitude. Not only can SKA find ~ 10 GL systems comparable to B1600+434 per day using its higher resolution, larger bandwidth and continuous monitoring capabilities (because of the multi-beam setup), we have also shown that microlensing, scintillation and intrinsic variability can easily be separated in these systems. SKA will therefore be a unique instrument to study compact objects and their mass-function in galaxies and their dark-matter halo up to very high redshifts. The large increase in the microlensing rate (a factor ≥ 1000 compared with stationary optical sources) for lensed flat-spectrum radio sources with superluminal components makes this a nearly impossible task for any optical telescope.

References

- [1] Alcock, C., et al. 1997, ApJ, 486, 697
- [2] Browne, I.W.A, et al., 1998, In "Observational Cosmology with the new radio surveys", Astrophysics and Space Science Library, Vol. 226, M. Bremer, Jackson, N. J. I. Phrez-Fournon, (eds.), Dordrecht: Kluwer Academic Publishers
- [3] Chengalur, J. N., De Bruyn, A. G. & Narasimha, D. 1999, A&A, 343, L79
- [4] Fassnacht, C.D., Cohen, J.G., 1998, AJ, 115, 377
- [5] Hopkins, A., Windhorst, R., Cram, L., Ekers, R., 1999, astro-ph/9906469
- [6] Ibata, R.A., Richer, H.B., Gilliland, R.L., Scott, D., 1999, astro-ph/9908270
- [7] Jackson, N., et al., 1995, MNRAS, 274, L25
- [8] Jaunsen, A.O., Hjorth, J., 1997, A&A, 317, L39
- [9] Koopmans, L.V.E., de Bruyn, A.G., Jackson, N., 1998, MNRAS, 295, 534
- [10] Koopmans, L.V.E., de Bruyn, A.G., Xanthopoulos, E., Fassnacht, C.D., 1999, A&A, submitted
- [11] Koopmans, L.V.E., de Bruyn, A.G., 1999, A&A, submitted
- [12] Mao, S. 1999, astro-ph/9909302
- [13] Méndez, R.A., Minniti, D., 1999, astro-ph/9908330
- [14] Paczynski, B. 1986, ApJ, 304, 1
- [15] Rickett, B.J., 1999, ARA&A, 28, 561
- [16] SKA scientific case, <http://www.nfra.nl/skai/science/>
- [17] Subramanian, K. & Gopal-Krishna 1991, A&A, 248, 55
- [18] Vermeulen, R. C. & Cohen, M. H. 1994, ApJ, 430, 467
- [19] Wambsganss, J., 1990, PhD thesis, Max-Planck-Institute für Physik und Astrophysik, MPA 550 October 1990